

# Crystal structure and aqueous solubility of ammonium D-glucarate

Ranko P. Bontchev\* and Robert C. Moore

Sandia National Laboratories, PO Box 5800, MS 0779 Albuquerque, NM 87185-0779, United States

Received 7 April 2005; accepted 21 June 2005

Available online 25 July 2005

**Abstract**—Ammonium D-glucarate,  $\text{NH}_4(\text{C}_6\text{H}_9\text{O}_8)$  [ammonium D-saccharate,  $\text{NH}_4\text{-SAC}$ ], has been synthesized, and its crystal structure solved by single-crystal X-ray diffraction methods.  $\text{NH}_4\text{-SAC}$  crystallizes in the monoclinic space group  $P2_1$  (#4) with cell parameters  $a = 4.8350(4) \text{ \AA}$ ,  $b = 11.0477(8) \text{ \AA}$ ,  $c = 16.7268(12) \text{ \AA}$ ,  $\beta = 90.973(1)^\circ$ ,  $V = 894.34(12) \text{ \AA}^3$ ,  $Z = 3$ . The structure was refined by full-matrix least-squares on  $F^2$  yielding final  $R$ -values (all data)  $R1 = 0.0353$  and  $R_w2 = 0.0870$ . The structure consists of alternating  $(\text{NH}_4)^+$  and  $(\text{C}_6\text{H}_{11}\text{O}_6)^-$  layers parallel to the  $bc$  plane. An extended network of  $\text{N-H}\cdots\text{O}_{\text{SAC}}$  and  $\text{O}_{\text{SAC}}\text{-H}\cdots\text{O}_{\text{SAC}}$  hydrogen bonds provide the 3-D connectivity. The aqueous solubility ( $S_w$ ) has been shown to be pH independent at ambient conditions within the range  $4.5 < \text{pH} < 10$  with  $S_w = 2.19 \text{ M/L}$ , whose value is about a factor of two lower than that of the ammonium isosaccharate analogue.

© 2005 Elsevier Ltd. All rights reserved.

**Keywords:** Crystal structure; Ammonium; Glucarate; Saccharate; Aqueous solubility

## 1. Introduction

Recent studies have shown that some natural sugars and their derivatives could be successfully used as components in formulations designed for heavy metal and radionuclides extraction from soils and urban materials.<sup>1–5</sup> It has also been shown that these strong chelating agents enhance the aqueous solubility of radionuclides in high oxidation states such as  $\text{Np(IV)}$  and  $\text{Th(IV)}$  by several orders of magnitude and have a significant effect on the reduction and sorption of Th and Pu by concrete surfaces.<sup>4,5</sup>

A typical example of such carbohydrates is D-glucaric (saccharic) acid. It has been shown that it has a strong complexing affinity towards the lanthanides  $\text{Ln(III)}$ ,  $\text{Mo(VI)}$ ,  $\text{W(VI)}$  and  $\text{Tc(IV)}$ .<sup>6–8</sup> Similar affinity has been demonstrated for some transition metals, the resulting structures varying from one-dimensional in

$\text{Cu(II)-SAC}$  to a 3-D open framework in  $\text{Zn(II)-SAC}$ .<sup>9,10</sup> A number of inorganic salts such as  $\text{Ca-SAC}$ ,  $\text{K-SAC}$  and  $\text{Na-SAC}$  have also been reported.<sup>11–13</sup>

The goal of our ongoing programme is the development of a new generation of carbohydrate-based decontaminating agents. We focus on new highly soluble biodegradable carbohydrate derivatives with high complexing ability.<sup>14,15</sup> In this paper, we report the synthesis, crystal structure and aqueous solubility of another inorganic D-saccharic acid derivative, ammonium saccharate ( $\text{NH}_4\text{-SAC}$ ).

## 2. Experimental

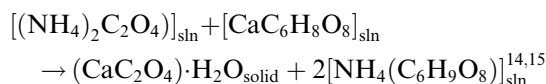
### 2.1. Materials

All chemicals were of analytical grade (Fisher Chemical Co.). Solutions were prepared using deionized water from a Barnstead Nanopure Water Purification System.

\* Corresponding author. Tel.: +1 505 845 0361; fax: +1 505 844 2348; e-mail: [rpbonc@sandia.gov](mailto:rpbonc@sandia.gov)

## 2.2. Synthesis

NH<sub>4</sub>–SAC was prepared using the previously described method based on ammonium oxalate and calcium saccharate:



After filtering the CaC<sub>2</sub>O<sub>4</sub> solid precipitate, the filtrate was evaporated at lowered pressure and temperature in a freeze-dry unit until white crystals formed at the bottom of the flask. Powder XRD analysis of the product did not show any traces of the starting Ca–SAC or any other impurity phases. Large enough single crystals of NH<sub>4</sub>–SAC were grown by slow evaporation of concentrated Na–ISA water solution at room temperature and pressure.

## 2.3. Physical measurements

The purity of a number of NH<sub>4</sub>–SAC syntheses was routinely monitored by powder X-ray diffraction (XRD) using a Bruker D8 Advance instrument with monochromatized Cu K $\alpha$  radiation. All lines in the powder XRD patterns were indexed using the structural model and cell parameters described below, and no impurity phases have been detected. A typical powder XRD pattern is shown in Figure 1.

Infrared spectra were recorded on a Perkin–Elmer Spectrum One spectrometer within the range 400–4000 cm<sup>−1</sup> using the KBr pellet method. The FTIR spectrum of NH<sub>4</sub>–SAC consists of the typical C–O, C–C, C–H and O–H vibrations along with the most characteristic NH<sub>4</sub> band at ca. 1400 cm<sup>−1</sup> (Fig. 2).<sup>14–16</sup>

## 2.4. Structure determination

A colourless polyhedral crystal of NH<sub>4</sub>–SAC was mounted on a SIEMENS SMART X-ray diffractometer

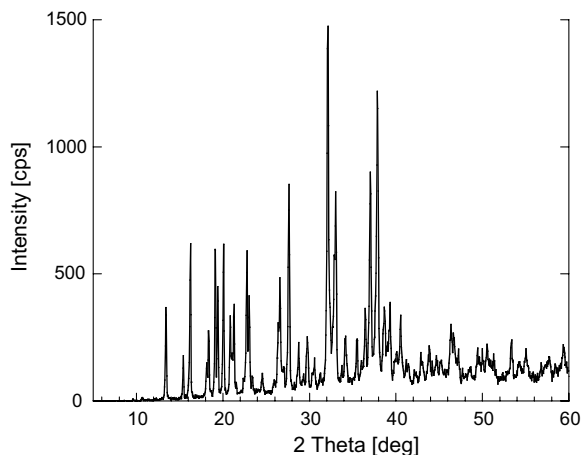


Figure 1. Powder XRD pattern of NH<sub>4</sub>–SAC.

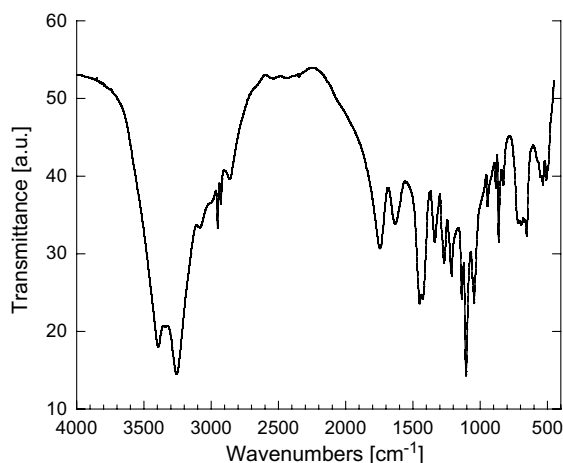


Figure 2. FTIR spectrum of NH<sub>4</sub>–SAC.

with a 1K CCD area detector. Data were collected at room temperature using graphite-monochromatized Mo K $\alpha$  radiation ( $\lambda = 0.71073 \text{ \AA}$ ). A hemisphere of data (1271 frames at 5-cm detector distance) was collected using a narrow-frame method with scan widths of  $0.30^\circ$  in  $\omega$  and an exposure time of 30 s/frame. The data were integrated using the Siemens SAINT program.<sup>17</sup> The program SADABS was used for the absorption correction.<sup>18</sup> The structure was solved by direct methods and refined by full matrix least-squares techniques with the SHELX97 software package.<sup>19</sup> The main crystallographic details are summarized in Table 1.

Table 1. Crystal data and structure refinement for NH<sub>4</sub>–SAC

Empirical formula	C <sub>8</sub> H <sub>17.33</sub> N <sub>1.33</sub> O <sub>10.67</sub>
Formula weight	302.90
Temperature	293(2) K
Wavelength	0.71073 Å
Crystal system, space group	Monoclinic, S.G. <i>P</i> 2 <sub>1</sub> (#4)
Unit cell dimensions	<i>a</i> = 4.8350(4) Å; $\alpha$ = $90^\circ$ <i>b</i> = 11.0477(8) Å; $\beta$ = 90.973(1) $^\circ$ <i>c</i> = 16.7268(12) Å; $\gamma$ = $90^\circ$
Volume, <i>Z</i>	893.34(12) Å <sup>3</sup> , 3
Calculated density	1.689 g cm <sup>−3</sup>
Absorption coefficient	0.160 mm <sup>−1</sup>
<i>F</i> (000)	480
Crystal size	0.30 × 0.13 × 0.09 mm
$\theta$ Range for data collection	1.22–30.04 $^\circ$
Limiting indices	−6 ≤ <i>h</i> ≤ 6, −15 ≤ <i>k</i> ≤ 14, −23 ≤ <i>l</i> ≤ 23
Reflections collected/unique	10,399/4980 [ <i>R</i> (int) = 0.0202]
Refinement method	Full-matrix least-squares on <i>F</i> <sup>2</sup>
Data/parameters	4980/376
Goodness-of-fit on <i>F</i> <sup>2</sup>	0.998
Final <i>R</i> indices [ <i>I</i> > 2 $\sigma$ ( <i>I</i> )]	<sup>a</sup> <i>R</i> 1 = 0.0338, <sup>b</sup> <i>R</i> <sub>w</sub> 2 = 0.0856
<i>R</i> indices (all data)	<i>R</i> 1 = 0.0353, <i>R</i> <sub>w</sub> 2 = 0.0870
Largest diff. peak and hole	0.470 and −0.251 e Å <sup>−3</sup>

<sup>a</sup> *R*1 =  $\Sigma||F_o| - |F_c|/\Sigma|F_o|$  (based on reflections with *I* > 2 $\sigma$ (*I*)).

<sup>b</sup> *R*<sub>w</sub> =  $[\Sigma w(|F_o| - |F_c|)^2 / \Sigma w|F_o|^2]^{1/2}$ ;  $w = 1/[\sigma^2(F_o^2) + (0.629P)^2 + 0.01P]$ ; *P* =  $[\text{Max}(F_o^2, 0) + 2F_c^2]/3$  (all data).

The observed Laue symmetry and reflection conditions ( $0k0$ ;  $k = 2n$ ) were indicative of the monoclinic

**Table 2.** Atomic coordinates ( $\times 10^4$ ) and equivalent isotropic displacement parameters ( $\text{\AA}^2 \times 10^3$ ) for  $\text{NH}_4\text{-SAC}$ .  $U(\text{equiv})$  is defined as one third of the trace of the orthogonalized  $U_{ij}$  tensor

Atom	<i>x</i>	<i>y</i>	<i>z</i>	$U(\text{equiv})$
C(1)	3927(2)	7167(1)	6022(1)	9(1)
C(2)	6015(2)	6284(1)	6395(1)	8(1)
C(3)	4579(2)	5370(1)	6949(1)	8(1)
C(4)	2972(2)	4363(1)	6522(1)	8(1)
C(5)	4798(2)	3536(1)	6010(1)	8(1)
C(6)	2922(2)	2584(1)	5610(1)	9(1)
C(7)	6100(2)	2076(1)	9194(1)	9(1)
C(8)	3967(2)	1309(1)	8726(1)	8(1)
C(9)	5413(2)	532(1)	8088(1)	8(1)
C(10)	7159(2)	9483(1)	8416(1)	8(1)
C(11)	5382(2)	8534(1)	8842(1)	8(1)
C(12)	7260(3)	7528(1)	9159(1)	10(1)
O(1)	2346(2)	6639(1)	5478(1)	11(1)
O(2)	3790(2)	8221(1)	6231(1)	13(1)
O(3)	8087(2)	6918(1)	6826(1)	11(1)
O(4)	2805(2)	5997(1)	7487(1)	10(1)
O(5)	1749(2)	3650(1)	7134(1)	10(1)
O(6)	6928(2)	2983(1)	6471(1)	10(1)
O(7)	2998(2)	1519(1)	5846(1)	12(1)
O(8)	1323(2)	3013(1)	5062(1)	11(1)
O(9)	6292(2)	3177(1)	9053(1)	12(1)
O(10)	7592(2)	1486(1)	9697(1)	11(1)
O(11)	1917(2)	2043(1)	8351(1)	9(1)
O(12)	7043(2)	1300(1)	7600(1)	10(1)
O(13)	8490(2)	8946(1)	7746(1)	10(1)
O(14)	3308(2)	8066(1)	8327(1)	12(1)
O(15)	8908(2)	7938(1)	9730(1)	13(1)
O(16)	7182(2)	6506(1)	8897(1)	15(1)
N(1)	8249(2)	30(1)	6046(1)	11(1)
N(2)	1587(2)	4681(1)	8967(1)	11(1)
H(1)	3110(30)	833(17)	9120(10)	6(4)
H(2)	6940(40)	5896(18)	5955(11)	13(4)
H(3)	5940(30)	4984(15)	7267(10)	4(4)
H(4)	5730(30)	3953(17)	5615(10)	9(4)
H(5)	6840(40)	10437(17)	5965(11)	15(4)
H(6)	4070(40)	229(15)	7738(10)	6(4)
H(7)	8550(30)	9806(15)	8776(9)	7(3)
H(8)	1690(40)	5193(19)	9341(12)	22(5)
H(9)	4490(30)	8870(16)	9294(10)	7(4)
H(10)	1490(30)	4696(16)	6182(10)	7(4)
H(11)	8450(40)	1530(20)	7841(12)	25(5)
H(12)	230(50)	3530(20)	6965(13)	30(6)
H(13)	9760(40)	10491(18)	5955(12)	21(5)
H(14)	1340(50)	6200(20)	7247(13)	32(6)
H(15)	1670(40)	5050(20)	8551(13)	22(5)
H(16)	8250(40)	9780(20)	6497(13)	23(5)
H(17)	8360(40)	9421(18)	5742(11)	16(4)
H(18)	2840(40)	4165(18)	8989(10)	14(4)
H(19)	9970(40)	8794(18)	7908(12)	17(5)
H(20)	9960(40)	4305(19)	9015(12)	31(5)
H(21)	2660(40)	2440(20)	8014(12)	15(5)
H(22)	7560(40)	7450(20)	7038(13)	18(5)
H(23)	3630(50)	7460(20)	8173(14)	27(6)
H(24)	6430(50)	2490(20)	6776(14)	23(5)
H(25)	9710(50)	2220(20)	12(16)	49(7)
H(26)	870(50)	7190(30)	5268(15)	51(7)

space groups  $P2_1$  (#4) and  $P2_1/m$  (#11). A comparison of the initial solutions in both space groups indicated low symmetry, and the structure was refined successfully using the low-symmetry model in S.G.  $P2_1$ . Initially all nonhydrogen atoms were located and assigned, and their thermal parameters were refined anisotropically. Next, all hydrogen atoms were located directly from the difference Fourier map and refined with isotropic thermal parameters. After the refinement converged, a close examination of the solution, as well as a test using the PLATON program, confirmed the lack of possible higher symmetry.<sup>20</sup> Atomic coordinates and isotropic thermal parameters are listed in Table 2.

## 2.5. Aqueous solubility

Solubility measurements were carried out within the range  $4.5 < \text{pH} < 10$  following the procedure described before.<sup>14,15</sup> The pH was adjusted by adding  $\text{NH}_4\text{OH}$  and/or  $\text{HCl}$ , and the samples were left to equilibrate for two weeks at room temperature. After filtration of the liquid, 1.00 mL of each saturated solution was transferred to a small aluminum tray, weighed and let dry at 30 °C for another week. The dry products were weighed again, and the molar solubility was calculated based on the weight difference between the saturated solutions and the dried products. Powder XRD and FTIR analyses confirmed that all dried samples correspond to well crystallized  $\text{NH}_4\text{-SAC}$ . Two control samples were processed in the same way after equilibrating for 4 weeks. The results matched the linear fit of the water solubilities of the two-week equilibrated series.

## 3. Results and discussion

### 3.1. Description of the structure

The asymmetric unit of  $\text{NH}_4\text{-SAC}$  consists of two crystallographically independent  $(\text{C}_6\text{H}_9\text{O}_8)^-$  anions,  $(\text{SAC})^-$ , charge balanced by two ammonium cations (Fig. 3). The 3-D structure is built up from  $(\text{C}_6\text{H}_9\text{O}_8)^-$  anions which are arranged in slabs parallel to the  $bc$  plane. The charge balance is provided by  $\text{NH}_4^+$  cations that are located in the space between the  $\text{SAC}^-$  slabs (Fig. 4). The main C–C and C–O distances and angles, listed in Table 3, are very close to those previously reported for K– and Na–SAC.<sup>12,13</sup>

A very complex network of hydrogen bonds links the  $(\text{ISA})^-$  and  $\text{NH}_4^+$  units and provides the 3-D connectivity (Fig. 5, Table 4; only intermolecular  $\text{A} \cdots \text{H}$  bonds with  $d \leq 2.2$  Å have been considered). Three of the hydrogen atoms of each  $\text{N}(1)\text{H}_4^+$  (H13, H5, H17) form three  $\text{N} \cdots \text{H} \cdots \text{O}$  bonds with two of the oxygen atoms of three different  $\text{SAC}^-$  species (2O7, O8) (Fig. 5 (top), Table 4). The last one, H16, is too far away from the

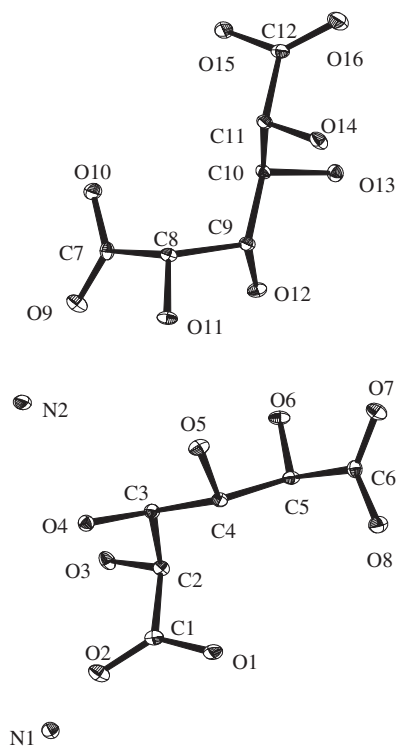


Figure 3. Asymmetric unit, 50% thermal ellipsoids, in  $\text{NH}_4\text{-SAC}$ .

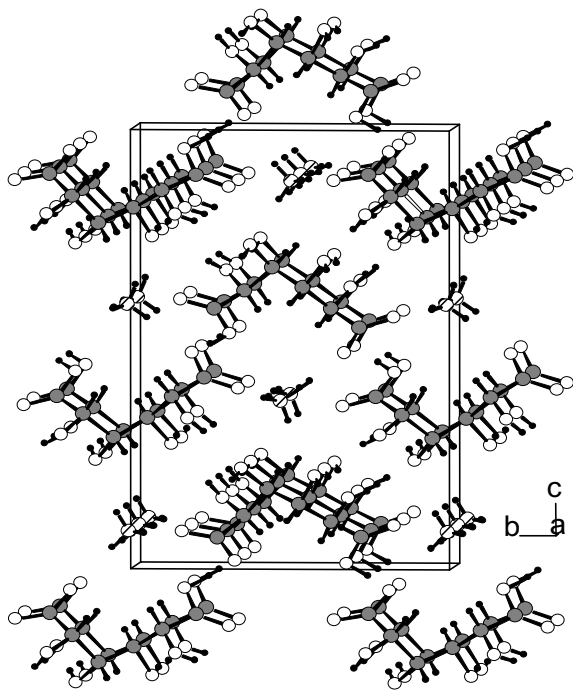


Figure 4. Unit cell and 3-D packing in  $\text{NH}_4\text{-SAC}$ . The atoms in the structure are drawn as the following circles: nitrogen (cross-hatched), carbon (filled), oxygen (white) and hydrogen (black).

closest oxygen atom and thus does not contribute to the H-bond network. The second crystallographically independent ammonium cation forms four different  $\text{N}\cdots\text{H}\cdots\text{O}_{\text{SAC}}$  hydrogen bonds through all four of the hydro-

Table 3. Selected bond lengths [Å] and angles [°] for  $\text{NH}_4\text{-SAC}$

O(1)–C(1)	1.3142(15)
O(2)–C(1)	1.2178(16)
O(3)–C(2)	1.4110(14)
O(4)–C(3)	1.4332(15)
O(5)–C(4)	1.4268(15)
O(6)–C(5)	1.4141(14)
O(7)–C(6)	1.2414(16)
O(8)–C(6)	1.2794(15)
O(9)–C(7)	1.2419(17)
O(10)–C(7)	1.2786(15)
O(11)–C(8)	1.4179(14)
O(12)–C(9)	1.4244(15)
O(13)–C(10)	1.4311(15)
O(14)–C(11)	1.4102(14)
O(15)–C(12)	1.3142(15)
O(16)–C(12)	1.2120(16)
C(1)–C(2)	1.5288(17)
C(2)–C(3)	1.5432(17)
C(3)–C(4)	1.5269(17)
C(4)–C(5)	1.5410(17)
C(5)–C(6)	1.5347(17)
C(7)–C(8)	1.5386(17)
C(8)–C(9)	1.5465(17)
C(9)–C(10)	1.5296(17)
C(10)–C(11)	1.5296(17)
C(10)–C(11)	1.5385(17)
C(11)–C(12)	1.5241(17)
O(2)–C(1)–O(1)	126.07(11)
O(2)–C(1)–C(2)	122.11(11)
O(1)–C(1)–C(2)	111.81(11)
O(3)–C(2)–C(1)	110.49(10)
O(3)–C(2)–C(3)	109.93(10)
C(1)–C(2)–C(3)	111.21(10)
O(4)–C(3)–C(2)	109.89(9)
O(4)–C(3)–C(4)	109.95(10)
C(2)–C(3)–C(4)	115.31(10)
O(5)–C(4)–C(3)	106.34(9)
O(5)–C(4)–C(5)	108.66(10)
C(3)–C(4)–C(5)	113.55(10)
O(6)–C(5)–C(4)	111.21(10)
O(6)–C(5)–C(6)	111.81(10)
C(4)–C(5)–C(6)	107.97(9)
O(7)–C(6)–O(8)	126.38(11)
O(7)–C(6)–C(5)	119.74(11)
O(8)–C(6)–C(5)	113.83(11)
O(9)–C(7)–O(10)	125.52(11)
O(9)–C(7)–C(8)	119.63(11)
O(10)–C(7)–C(8)	114.83(11)
O(11)–C(8)–C(7)	111.55(10)
O(11)–C(8)–C(9)	109.45(10)
C(7)–C(8)–C(9)	110.46(9)
O(12)–C(9)–C(8)	110.46(10)
O(12)–C(9)–C(10)	109.02(10)
C(8)–C(9)–C(10)	115.21(10)
O(13)–C(10)–C(9)	106.59(9)
O(13)–C(10)–C(11)	110.05(10)
C(9)–C(10)–C(11)	111.93(10)
O(14)–C(11)–C(10)	110.95(10)
O(14)–C(11)–C(12)	111.30(10)
C(10)–C(11)–C(12)	108.90(10)
O(16)–C(12)–O(15)	126.75(12)
O(16)–C(12)–C(11)	122.66(11)
O(15)–C(12)–C(11)	110.58(11)

Symmetry transformations used to generate equivalent atoms: #1  $x, y - 1, z$ ; #2  $x, y + 1, z$ .

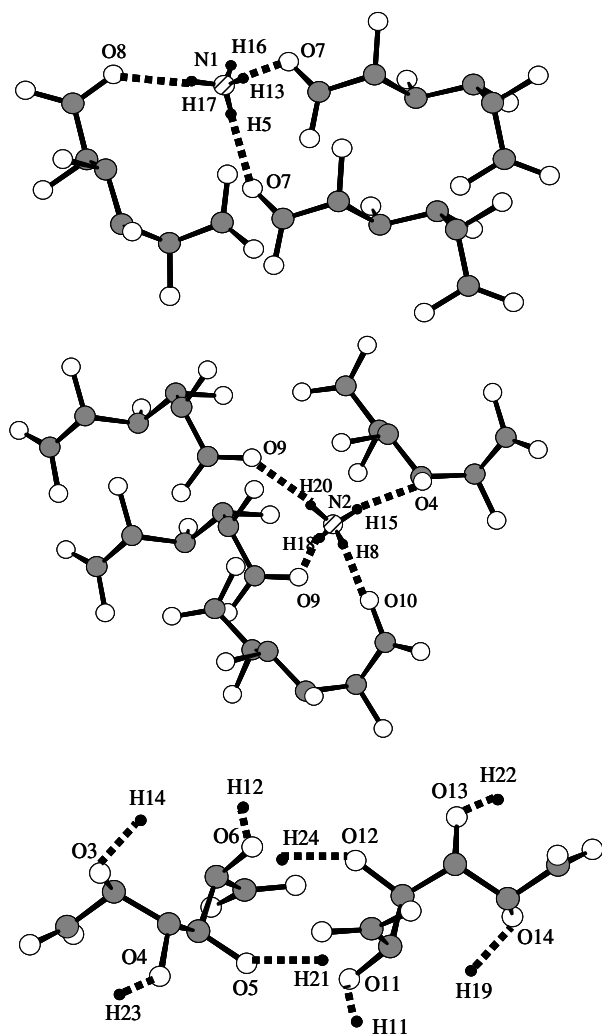


Figure 5. Hydrogen bonds (dotted lines) in  $\text{NH}_4\text{-SAC}$ .

Table 4. Hydrogen bonds [ $\text{\AA}$ ] in  $\text{NH}_4\text{-SAC}$

D–H...A	$d(\text{D–H})$	$d(\text{H...A})$
N1–H(13)...O(7)	0.90(2)	1.95(2)
N1–H(17)...O(8)	0.85(2)	2.06(2)
N1–H(5)...O(7)	0.83(2)	2.21(2)
N2–H(15)...O(4)	0.81(2)	2.14(2)
N2–H(8)...O(10)	0.85(2)	2.17(2)
N2–H(18)...O(9)	0.83(2)	2.00(2)
N2–H(20)...O(9)	0.89(2)	2.17(2)
O(4)–H(14)...O(3)	0.84(2)	1.89(2)
O(14)–H(23)...O(4)	0.73(2)	2.02(2)
O(5)–H(12)...O(6)	0.79(2)	1.88(2)
O(11)–H(21)...O(5)	0.81(2)	2.03(2)
O(6)–H(24)...O(12)	0.79(2)	1.92(2)
O(3)–H(22)...O(13)	0.73(2)	2.08(2)
O(13)–H(19)...O(14)	0.78(2)	1.93(2)
O(12)–H(11)...O(11)	0.82(2)	1.95(2)

gen atoms (Fig. 5 (middle), Table 4). In each  $\text{SAC}^-$  anion the four skeletal oxygen atoms participate in intermolecular  $(\text{SAC})^-\cdots(\text{SAC})$  hydrogen bonds (Fig. 5

(bottom), Table 4). The oxygen atoms from the terminal free carboxylic acid do not participate in any hydrogen bonds, while the remaining two oxygen atoms from the deprotonated carboxylate groups participate in  $\text{O}\cdots\text{H–N}$  bonds with the ammonium cations (Fig. 5, Table 4).

The overall crystal structure of  $\text{NH}_4\text{-SAC}$  is very similar to that of  $\text{KH-SAC}$ , the ammonium and potassium cations occupying the same geometrical positions.<sup>12</sup> Both derivatives crystallize in the same space group ( $P2_1$ ) with very close values of the  $a$ - and  $b$ -parameters and  $\beta$  angle. However, the presence of  $\text{N–H}\cdots\text{O}$  bonds in  $\text{NH}_4\text{-SAC}$  leads to additional distortion of the  $(\text{SAC})^-/\text{A}^+$  ordering, which in turn results in doubling of the  $c$ -parameter and cell volume.<sup>12</sup>

### 3.2. Thermal stability and water solubility

$\text{NH}_4\text{-SAC}$  is stable and preserves its crystallinity up to 172–175 °C. Upon further heating in air it melts incongruently into a brown solid and completely decays to  $\text{NH}_3$ ,  $\text{CO}_2$  and an unidentified mixture of residual organics. Clearly this relatively high thermal stability is again due to the extended network of hydrogen bonds.

The aqueous solubility of  $\text{NH}_4\text{-SAC}$  is independent of pH over the range  $4.5 < \text{pH} < 10$  (Fig. 6). Linear fit of the experimental solubility data ( $S$ ,  $[\text{M/L}]$ ) yielded the following equation:

$$S_{\text{NH}_4\text{-SAC}} = 2.19 + 0.001(\text{pH}); R = 0.99$$

The aqueous solubility of  $\text{NH}_4\text{-SAC}$ ,  $S = 2.19 \text{ M/L}$ , is close to that of sodium isosaccharate ( $\text{Na-ISA}$ ,  $S = 1.81 \text{ M/L}$ ) and about one half of that of ammonium isosaccharate ( $\text{NH}_4\text{-ISA}$ ,  $S = 4.04 \text{ M/L}$ ).<sup>15</sup> The differences in solubility can be explained by examining the structural differences between these compounds. In  $\text{Na-ISA}$  there are  $\text{O}_{\text{ISA}}\text{--Na--O}_{\text{ISA}}$  coordination bonds

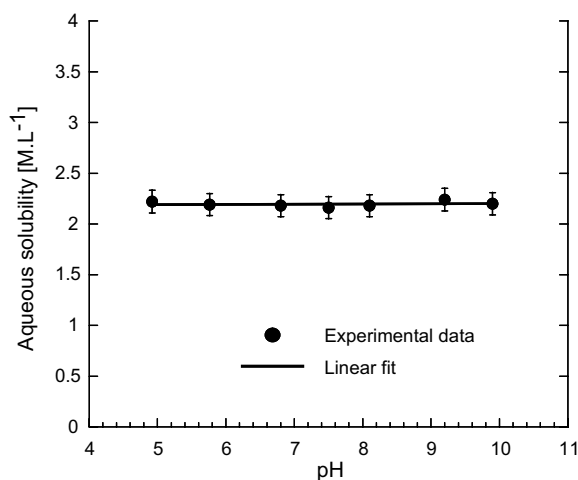


Figure 6. Aqueous solubility of  $\text{NH}_4\text{-SAC}$  as a function of pH at 20 °C.



which, although relatively weak, are still stronger than the corresponding  $\text{O}_{\text{ISA}} \cdots \text{H}-\text{N}-\text{H} \cdots \text{O}_{\text{ISA}}$  hydrogen bonds in  $\text{NH}_4\text{-ISA}$ .<sup>15</sup> On the other hand, the much more complicated and extended network of  $\text{O}_{\text{SAC}} \cdots \text{H}-\text{N}-\text{H} \cdots \text{O}_{\text{SAC}}$  and  $\text{O}_{\text{SAC}} \cdots \text{H}-\text{O}_{\text{SAC}}$  hydrogen bonds in  $\text{NH}_4\text{-SAC}$  leads to a decreased solubility, compared to that of  $\text{NH}_4\text{-ISA}$ . Although differing by a factor of two, both  $\text{NH}_4\text{-SAC}$  and  $\text{NH}_4\text{-ISA}$  show relatively high water solubility of the order of 2 and 4 M/L, respectively. In turn this makes them both excellent candidates for biodegradable complexing agents for radionuclide treatment and containment.

#### 4. Supplementary data

Full crystallographic details have been deposited in *cif*-format with the Cambridge Crystallographic Data Centre, CCDC No. 268035. Copies of this information could be obtained free of charge from the Director, CCDC, 12 Union Road, Cambridge, CB21EZ, UK, fax: +44 1223 336 033, e-mail: deposit@ccdc.cam.ac.uk; web: <http://www.ccdc.cam.ac.uk/conts/retrieving/html>.

#### Acknowledgements

Sandia is a multiprogram laboratory operated by Sandia Corporation, a Lockheed Martin Company, for the United States Department of Energy's National Nuclear Security Administration under contract DE-AC04-94AL85000.

#### References

1. Fischer, K.; Bipp, H.-P. *Water, Air Soil Pollut.* **2002**, *138*, 271.
2. Rai, D. P.; Rao, L. F.; Moore, D. A. *Radiochim. Acta* **1998**, *83*, 9.
3. Rai, D. P.; Rao, L. F.; Moore, D. A. *Radiochim. Acta* **1998**, *89*, 3.
4. Holgersson, S. Y.; Albinsson, B.; Allard, H.; Boren, I. *Radiochim. Acta* **1998**, *82*, 393.
5. Holt, K.; Moore, R. C.; Tucker, M.; Salas, F. *Rocky Mountain Regional ACS Meeting*, Albuquerque, NM, November, 2002.
6. Aury, S.; Rubini, P.; Gerardin, C.; Selve, C. *Eur. J. Org. Chem.* **2004**, 2057.
7. Ramos, M.; Caldeira, M.; Gil, V. *Inorg. Chim. Acta* **1991**, *180*, 219.
8. Yaoita, H.; Uehara, T.; Bronwell, A.; Rabito, C.; Ahmad, M.; Khaw, B.; Fischman, A.; Strauss, H. *J. Nucl. Med.* **1991**, *32*, 272.
9. Ferrier, F.; Avezou, A.; Terzian, G.; Benlian, D. *J. Mol. Struct.* **1998**, *442*, 281.
10. Abrahams, B.; Moylan, M.; Orchard, S.; Robson, R. *Angew. Chem., Int. Ed. Engl.* **2003**, *42*, 1848.
11. Burden, C.; Mackie, W.; Sheldrix, B. *Acta Crystallogr.* **1985**, *C41*, 693.
12. Taga, T.; Kuroda, Y.; Osaki, K. *Bull. Chem. Soc. Jpn.* **1977**, *50*, 3079.
13. Styron, S.; French, A.; Friedrich, J.; Lake, C.; Kiely, D. *J. Carbohydr. Chem.* **2002**, *21*, 27.
14. Bontchev, R. P.; Moore, R. C. *Carbohydr. Res.* **2004**, *339*, 801.
15. Bontchev, R. P.; Moore, R. C. *Carbohydr. Res.* **2004**, *339*, 2811.
16. Nakamoto, K. In *Infrared and Raman Spectroscopy of Inorganic and Coordination Compounds*, 5th ed.; John Wiley and Sons: New York, 1997.
17. Siemens Analytical X-ray Instruments; SAINT, Version 4.05, Madison, WI; 1995.
18. Sheldrix, G. M. *Program SADABS*; University of Göttingen, 1995.
19. Sheldrix, G. M. SHELX97 (Includes SHELXS97, SHELXL97, CIFTAB)—Programs for Crystal Structure Analysis (Release 97-2). Institut für Anorganische Chemie der Universität, Tammanstrasse 4, D-3400 Göttingen, Germany; 1998.
20. (a) Spek, A. L. *Acta Crystallogr., Sect. A* **1990**, *C34*, 46–57; (b) Spek, A. L. *PLATON. A Multipurpose Crystallographic Tool*; Utrecht University: Utrecht, 1998.